Chapter 17
LEAP-UCD-2017 Centrifuge Test at Kyoto University

Ruben R. Vargas, Tetsuo Tobita, Kyohei Ueda, and Hikaru Yatsugi

Abstract As part of the LEAP-UCD-2017 exercise, 24 centrifuge tests were conducted at 9 centrifuge facilities around the world; among them, 3 tests were carried out in the facilities of the Disaster Prevention Research Institute at Kyoto University. The main objective of the tests is to characterize the median response and uncertainty of the dynamic response of a uniform-density sloping deposit of clean sand, subjected to a ramped sinusoidal wave; this chapter introduces specific details of the model preparation, testing procedures, and achieved response. Additionally, a brief discussion related to the uncertainties in the density estimation is presented.

17.1 Introduction

During the past 40 years, efforts and developments in computational modeling of geo-materials have contributed significantly to increase the accuracy of prediction of the dynamic response of soil systems. Due the catastrophic consequences (as result of seismic events), special emphasis has been pointed to the liquefaction-induced ground failures. However, despite the efforts, results of numerical simulations have a certain degree of discrepancy with results obtained in physical modeling. Therefore, it is important to highlight that exercises of verification and validation (V&V) of numerical simulations are still needed to enhance the reliability of numerical models for liquefaction prediction.

Previous V&V works such as "VELACS Project" (1994) and "LEAP-GWU-2015" have attempted to verify numerical simulations in comparison to centrifuge experiments, but more efforts are needed prior to reaching definitive conclusions.

R. R. Vargas (✉) · K. Ueda
Disaster Prevention Research Institute, Kyoto University, Kyoto, Japan
e-mail: vargas.rodrigo.35m@st.kyoto-u.ac.jp

T. Tobita
Department of Civil Engineering, Kansai University, Osaka, Japan

H. Yatsugi
Faculty of Environmental and Urban Engineering, Kansai University, Osaka, Japan

B. Kutter et al. (eds.), *Model Tests and Numerical Simulations of Liquefaction and Lateral Spreading*, https://doi.org/10.1007/978-3-030-22818-7_17

LEAP (Liquefaction Experiments and Analysis Projects) is a joint project that pursues the verification, validation, and uncertainty quantification of numerical liquefaction models, based on centrifuge experiments. This project will have several exercises, in the sense that each one would be focused on different aspects of soil liquefaction, such as dams, ports, lateral spreading, etc.

"LEAP-UCD-2017" is one of the LEAP's exercises, whose main objective is to perform a sufficient number of experiments to characterize the median response, and the uncertainty of a specific sloping deposit of sand. Centrifuge experiments in nine facilities around the world were developed for this exercise; this paper will make a review of the experiments performed in the installations of the Disaster Prevention Research Institute (DPRI) at Kyoto University. Three experiments were performed; two of which (KyU2 and KyU3) are presented in this paper with emphasis on model preparation, testing process, and special features that may cause uncertainty or variations in comparison to experiments developed in other facilities.

17.2 Test Specifications and Model Preparation

17.2.1 Description of the Model and Instrumentation

Ottawa F-65 was chosen as standard sand for "LEAP-UCD-2017"; this sand was provided to the facilities by UC Davis (see details in Kutter et al. 2019). To avoid small errors due to uncertainty in specific gravity (Gs) and the maximum and minimum densities, the sand placement was prescribed based on target density (in replacement of relative density).

A uniform-density, 5-degree slope model inside a rigid container was specified for this exercise (see Fig. 17.1); a scaling ratio of 44.44 has been employed for the tests at Kyoto, which leads to prototype scale's dimensions to be 20 m in length, 4 m in height at midpoint, and 6.66 m of width.

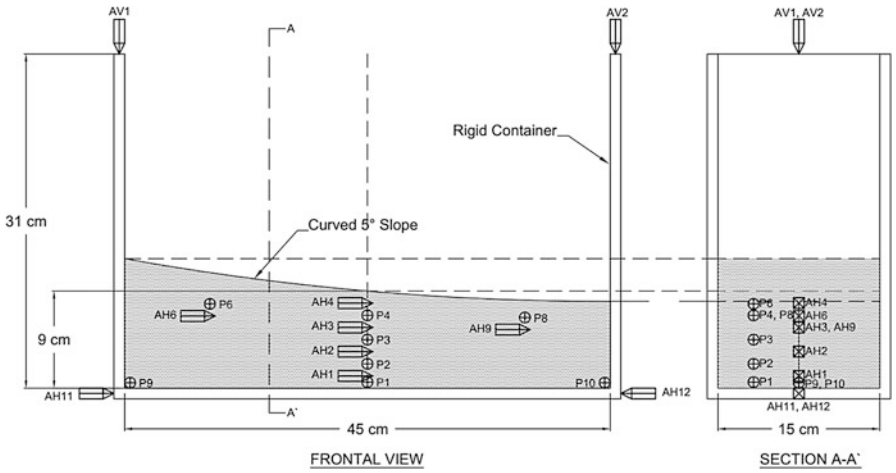

Fig. 17.1 Dimensions of the tested model

Regarding instrumentation of the model, nine horizontal accelerometers (AH1, AH2, AH3, AH4, AH6, AH9, AH11, and AH12), two vertical accelerometers (AV1 and AV2), and eight pore pressure transducers (P1, P2, P3, P4, P6, P8, P9, and P10) were placed.

17.2.2 Air Pluviation and Surface Curving

The specified technique for sand placement was air pluviation. A U.S. Standard Sieve No. 16 with a three-slot arrangement (each one of 100 mm x 10.3 mm) was specified as the pluviation tool (see Fig. 17.2).

During the sand placement (after height calibration), density was measured at three different stages in each model, using a rigid steel ruler (with a wood support). Achieved densities of 1659 and 1637 kg/m^3 were obtained for tests KyU2 and KyU3, respectively. A brief analysis about sensitivity and density measurement is presented in Sect. 17.4.

The centrifuge facility at Kyoto University has an effective radius of 2.50 m, and is equipped with a shaking table in the circumferential direction. In order to avoid errors due to variations in the radial gravity field (as stated by Tobita et al. 2018), the surface was curved according to the geometry of the facility; therefore, all points in the surface will have the same slope relative to the gravity field, and would represent ground with a constant, 5-degree slope angle in the prototype scale. In order to achieve the curved surface: (a) a flat specimen was obtained by air pluviation, (b) an aluminum guide was fabricated with the shape of the target curved surface, (c) a fixed length aluminum pipe is conditioned to a vacuum apparatus, and (d) following the guide, vacuum is applied to reach the curved surface (see Fig. 17.3).

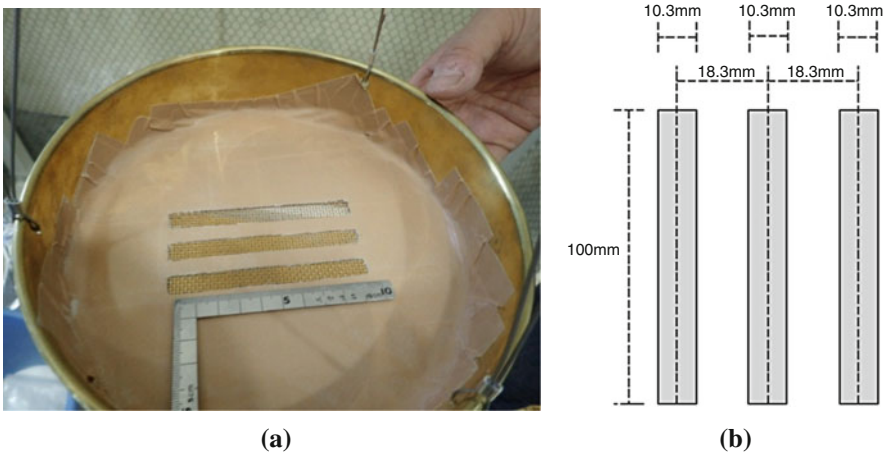

Fig. 17.2 (**a**) Tool employed for air pluviation procedure. (**b**) Geometry of the openings for the pluviation

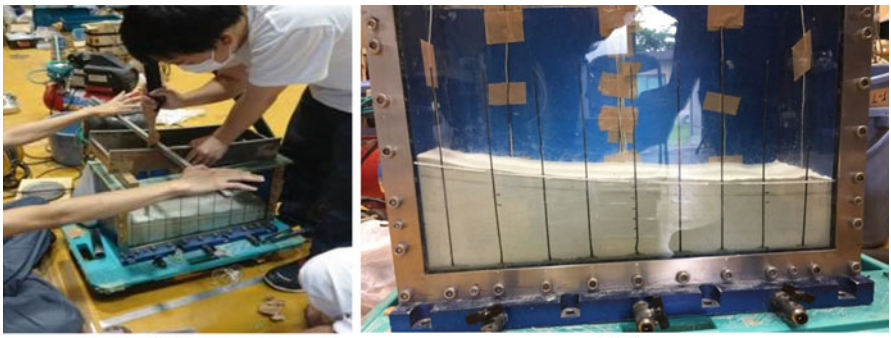

Fig. 17.3 (**a**) Vacuum process to obtain the curved surface. (**b**) Achieved curved surface

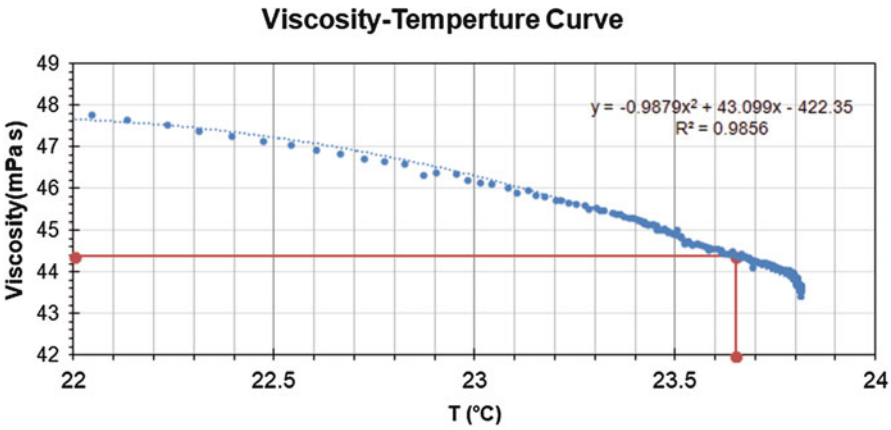

Fig. 17.4 Viscosity–temperature curve

17.2.3 Saturation, Input Motions, Measurement of Surface Deformations and Cone Penetration Testing (CPT)

After air pluviation and sensor placement, the rigid container was placed in a vacuum chamber, and one series of vacuum –CO_2– vacuum was applied in order to facilitate dissolution of gas bubbles, prior to saturation with a de-aired solution of Methylcellulose (SM-100, Shin'etsu Chemical Co.), following the method proposed by Okamura and Inoue (2012). Figure 17.4 shows the viscosity–temperature curve measured using a "Tuning-Fork Vibration Viscometer" (Izumo 2006).

The specified procedure includes a shake sequence of six input motions, which consists of ramped sinusoidal 1 Hz wave (as seen in Fig. 17.5a). Motions 2, 3, and

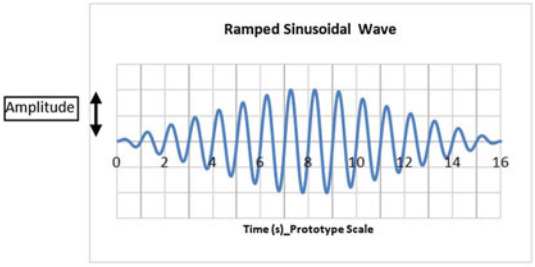

(a)

Motion	Amplitude (g)
Motion 1	0.015
Motion 2	0.15
Motion 3	0.25
Motion 4	0.015
Motion 5	0.25
Motion 6	0.015

(b)

Fig. 17.5 (**a**) Specified ramped sine wave. (**b**) Amplitude of motions

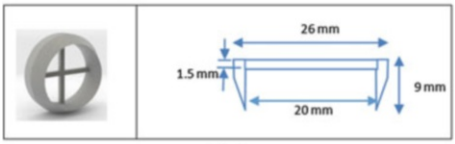

(a)

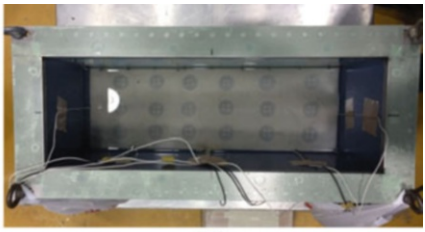

(b)

Fig. 17.6 (**a**) Geometry of surface markers. (**b**) Placement of surface markers

5 were considered as "destructive" and motions 1, 4, and 6 as "nondestructive" (see Fig. 17.5b).

Due to the presence of high-frequency vibrations in the achieved motions, and taking into account that higher frequency components have some but relatively small effect on the behavior of the model, this project (as a first approximation) used the effective PGA, defined as:

$$\mathrm{PGA}_{\mathrm{effective}} = \mathrm{PGA}_{1\mathrm{Hz}} + 0.5 \times \mathrm{PGA}_{\mathrm{hf}}$$

where: "$\mathrm{PGA}_{1\mathrm{Hz}}$" represents the PGA of the 1 Hz component of the achieved motion, and "$\mathrm{PGA}_{\mathrm{hf}}$" represents the higher frequency components of the ground motion.

To measure the surface displacements before and after each destructive motion, 18 surface markers provided by UC Davis were placed in the soil surface (see Fig. 17.6).

Additionally, three cone penetration tests in each experiment were performed (before each destructive motion) with a new 6 mm Mini-CPT provided by UC Davis; according to the specifications, the penetration rate was fixed as 2.12 mm/s.

17.3 Test Results

17.3.1 Achieved Ground Motions

As stated in the previous section, six input motions were applied to each model. For each destructive motion, PGA_{1Hz} values were calculated using a notched band pass filter with corner frequencies between 0.9 and 1.1 times the predominant frequency (i.e., 1 Hz). An example of the signal filtering process and the estimated values of $PGA_{effective}$ for destructive motions are shown in Fig. 17.7a.

As shown in Fig. 17.7b, in order to get experimental data to verify the concept of "effective PGA" (as defined in Sect. 17.2.3), a calibration for the motions was

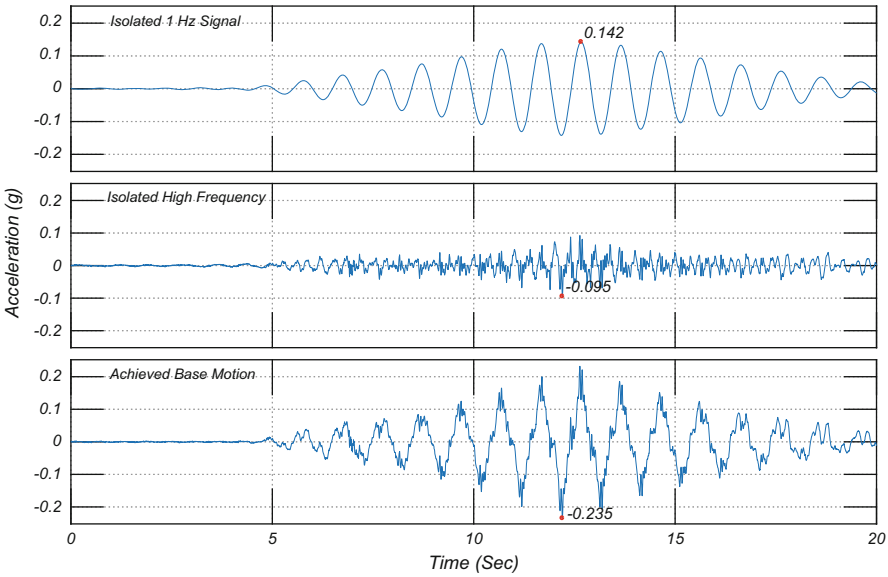

(a)

Motion		Target PGA (g)	Achieved PGA (g)	PGA of 1 Hz component (g)	Achieved PGA effective (g)
KyU2	Motion 2	0.15	0.12	0.10	0.11
	Motion 3	0.25	0.33	0.20	0.27
	Motion 5	0.25	0.33	0.21	0.27
KyU3	Motion 2	0.15	0.14	0.09	0.12
	Motion 3	0.25	0.24	0.14	0.19
	Motion 5	0.25	0.23	0.14	0.19

(b)

Fig. 17.7 (**a**) Filtering of input motion 3—KyU3. (**b**) Achieved input PGA

developed in the sense that, for the KyU2 Model the values of "achieved PGA effective" would be close to the target values, and in the KyU3 Model, the values of "achieved PGA" would be close to the target values.

In Fig. 17.8, the whole input motions (without any filtering process) are reported.

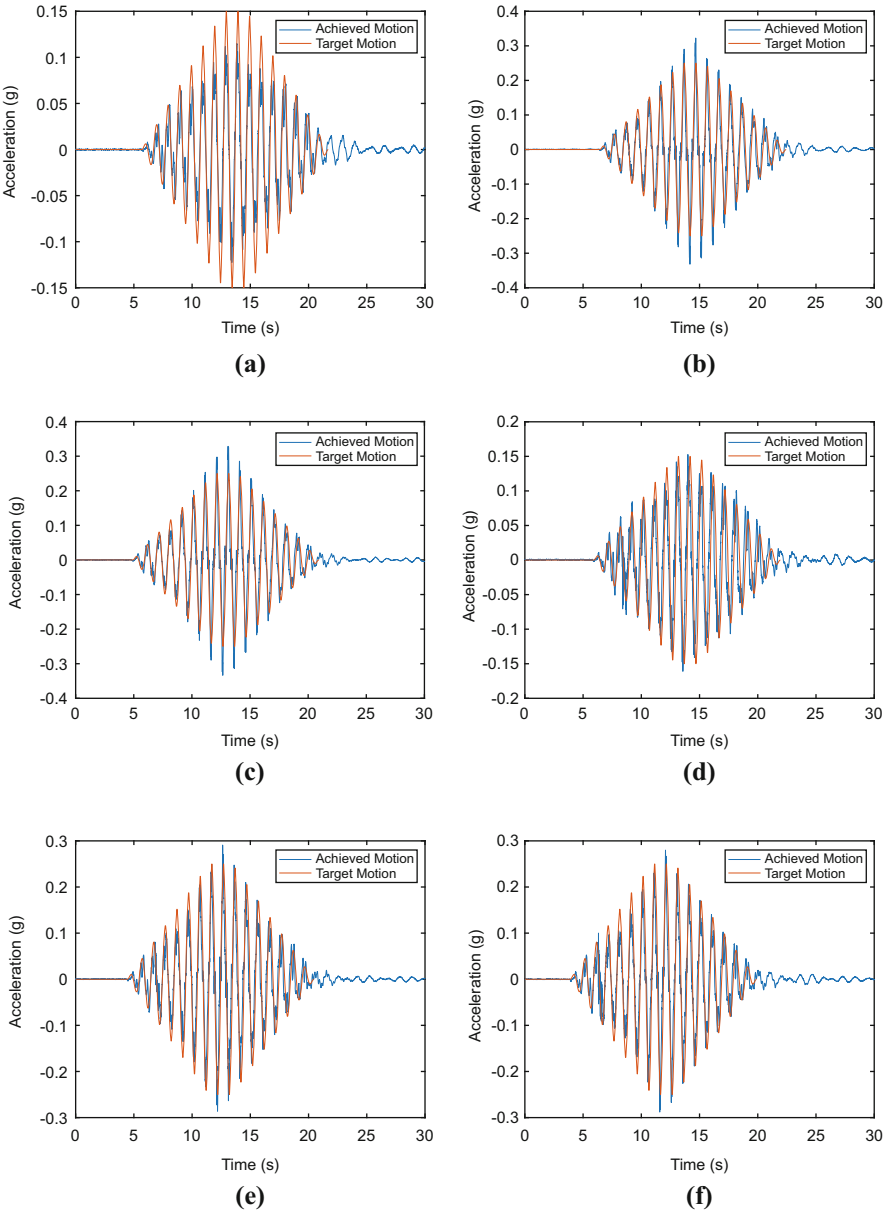

Fig. 17.8 (**a**) Input Motion-Motion 2-Model KyU2; (**b**) Input Motion-Motion 3-Model KyU2; (**c**) Input Motion-Motion 5-Model KyU2; (**d**) Input Motion-Motion 2-Model KyU3; (**e**) Input Motion-Motion 3-Model KyU3; (**f**) Input Motion-Motion 5-Model KyU3

17.3.2 Excess Pore Pressure During Motions

As specified, pore pressure transducers (PPTs) were employed to measure the increase of excess pore water pressure (Δu); in Fig. 17.9, the correspondent values of Δu and the initial values of effective vertical stress are presented for Model KyU2.

In this paper, the excess pore pressure ratio is defined as: $r_u = \Delta u / \sigma'_v$. Regarding Model KyU2, full liquefaction (i.e. $r_u \approx 1$) for Motion 2 (Fig. 17.9a) was only achieved in shallow parts (sensors P6, P4, and P8). Values of r_u between 0.75 and 0.9 were recorded for sensors P1, P2, P3, and P10; however, for sensor P9 a maximum value of r_u equal to 0.35 was observed. Records of sensors in Motion 3 (Fig. 17.9b) indicate that values of $r_u \approx 1$ were achieved also in sensors P4, P6, P8, and P10 (corresponding to shallow areas and the base of the downslope side), and values between 0.85 and 0.95 were reported in sensors P1, P2, and P3; for sensor P9,

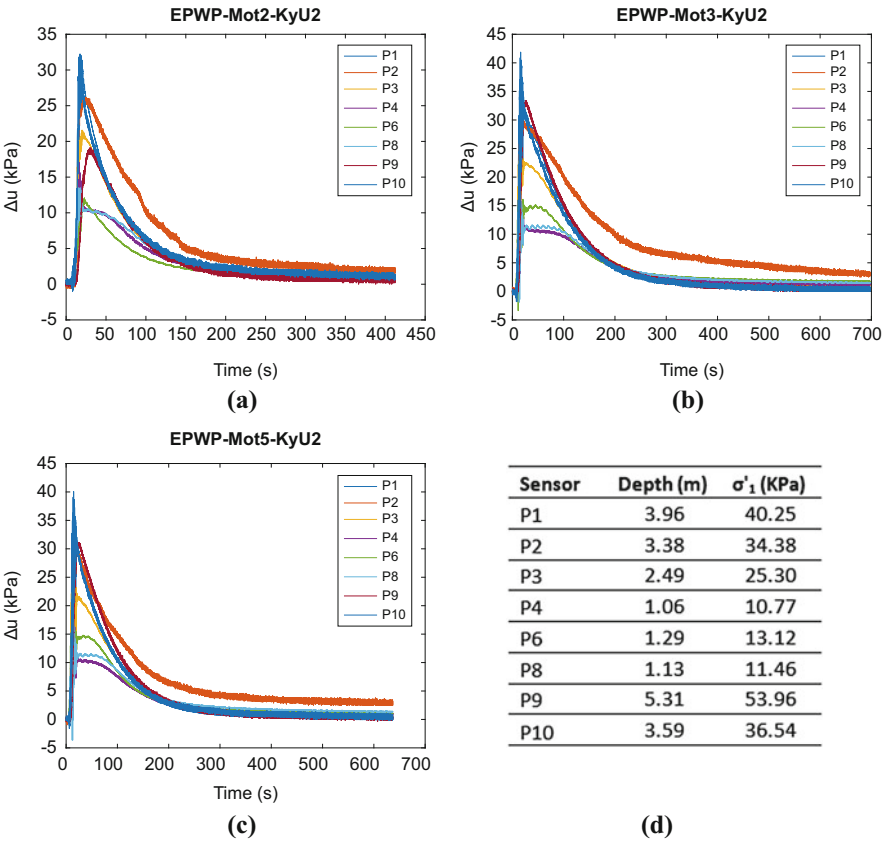

Sensor	Depth (m)	σ'_1 (KPa)
P1	3.96	40.25
P2	3.38	34.38
P3	2.49	25.30
P4	1.06	10.77
P6	1.29	13.12
P8	1.13	11.46
P9	5.31	53.96
P10	3.59	36.54

Fig. 17.9 (**a**) Excess pore water pressure motion 2—Model KyU2, (**b**) Excess pore water pressure motion 3—Model KyU2, (**c**) Excess pore water pressure motion 5—Model KyU2, (**d**) Initial stress state for sensors

a value of 0.60 was found. In case of Motion 5 (Fig. 17.9c), the behavior remained the same as the one described in Motion 3. It is important to mention that despite the increase in the values of q_c (obtained through the CPT test before Motion 3, and before Motion 5 (Fig. 17.17)), no increase in liquefaction resistance has been reported (with exception of sensors P1 and P9, where a small increase was recorded).

Regarding Model KyU3, it is important to mention that sensor P9 did not function during the test, so, its values will not be reported. For Motion 2 (Fig. 17.10a), full liquefaction (i.e. $r_u \approx 1$) was only achieved in the shallow part of the downslope (i.e. sensor P8); values of r_u under 0.70 were recorded in the bottom of the model (sensors P1 and P10), and values from 0.75 to 0.90 were obtained in sensors P2, P3, P4, and P6. Records of sensors in Motion 3 (Fig. 17.10b) indicate that values of $r_u \approx 1$ were achieved almost in all sensors, except in sensors P2 and P4, where a value of around 0.9 was found. In case of Motion 5 (Fig. 17.10c), the behavior of sensors P3, P4, P6, and P8 remained the same as the one described in Motion

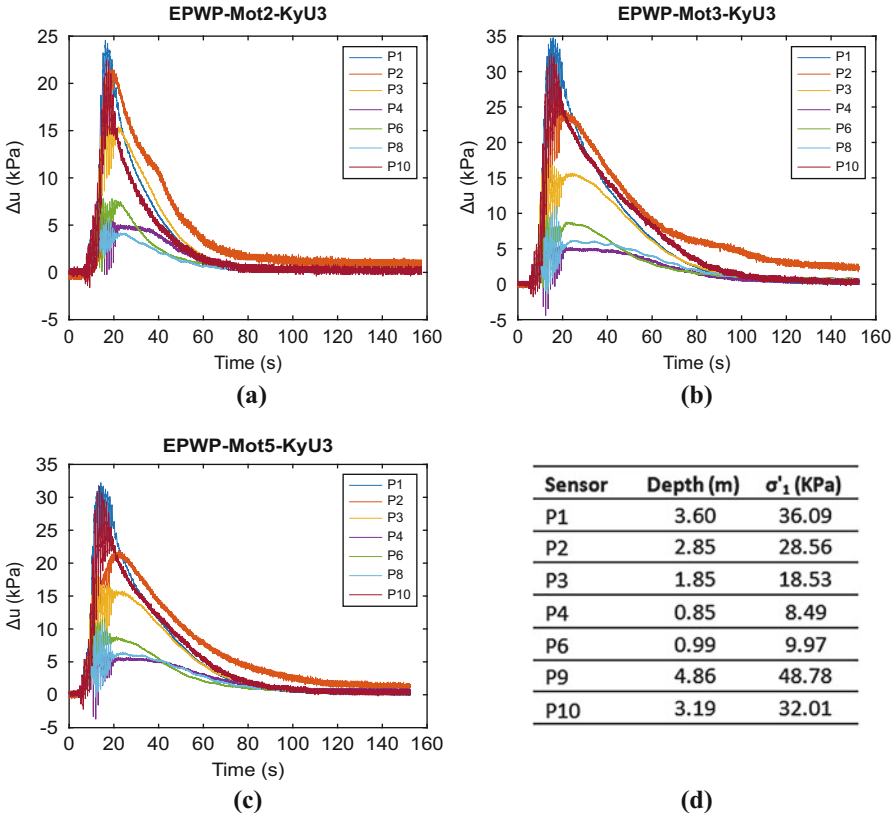

Sensor	Depth (m)	σ'₁ (KPa)
P1	3.60	36.09
P2	2.85	28.56
P3	1.85	18.53
P4	0.85	8.49
P6	0.99	9.97
P9	4.86	48.78
P10	3.19	32.01

(d)

Fig. 17.10 (**a**) Excess pore water pressure motion 2—Model KyU3. (**b**) Excess pore water pressure motion 3—Model KyU3. (**c**) Excess pore water pressure motion 5—Model KyU3. (**d**) Initial stress state for sensors

3. However, for sensors P1 and P2, a reduction in the r_u value of 7% and 15% respectively was found; in this model, no significant difference among values of qc (obtained through the CPT test before Motion 3, and before Motion 5) were reported (Fig. 17.17).

17.3.3 Ground Motion Accelerations

Response time histories for all accelerometers placed inside the deposit are reported in Figs. 17.11, 17.12, 17.13, 17.14, 17.15, and 17.16. As expected for the results of excess pore water pressure (EPWP), for both models, in Motion 2 (i.e. Fig. 17.11 and 17.14) neither significant amplification nor distortion has been recorded for the

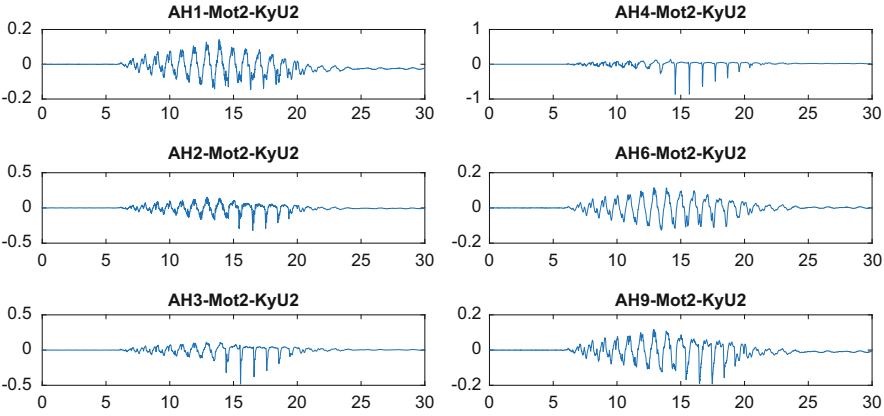

Fig. 17.11 Ground motion accelerations (g) versus time (s) for Model KyU2—Motion 2

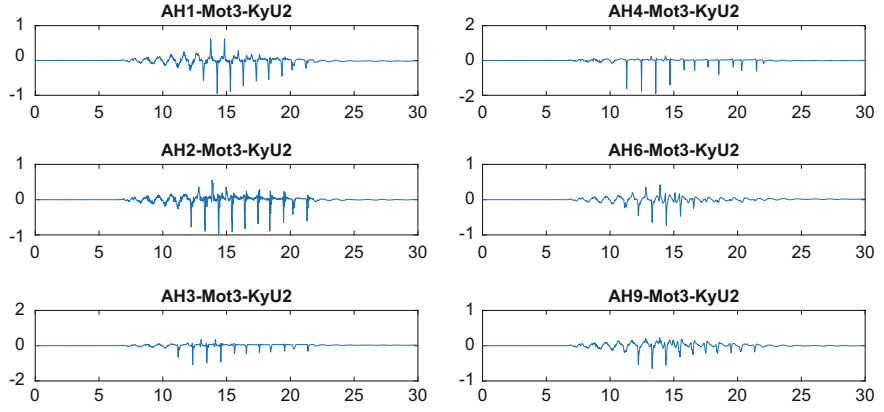

Fig. 17.12 Ground motion accelerations (g) versus time (s) for Model KyU2—Motion 3

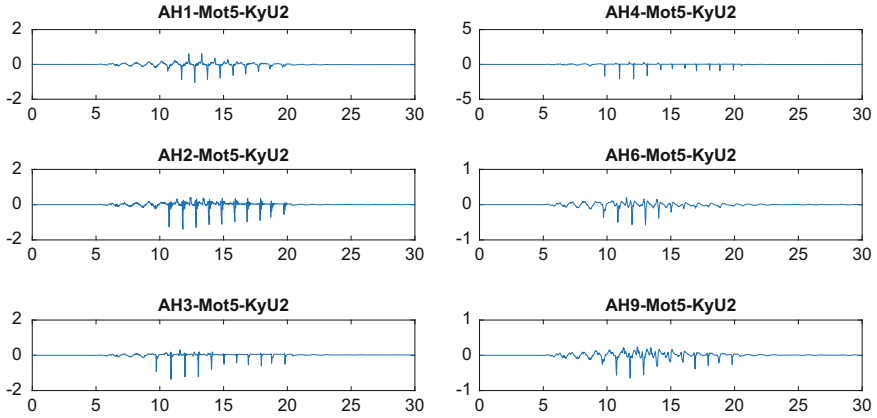

Fig. 17.13 Ground motion accelerations (g) versus time (s) for Model KyU2—Motion 5

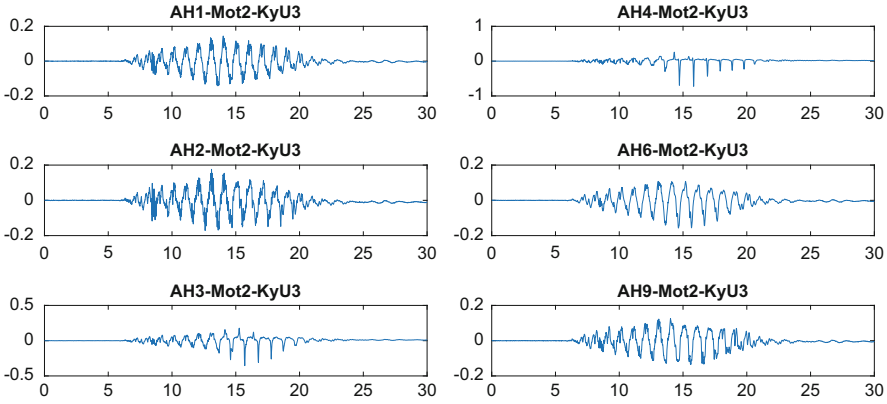

Fig. 17.14 ground motion accelerations (g) versus time (s) for Model KyU3—Motion 2

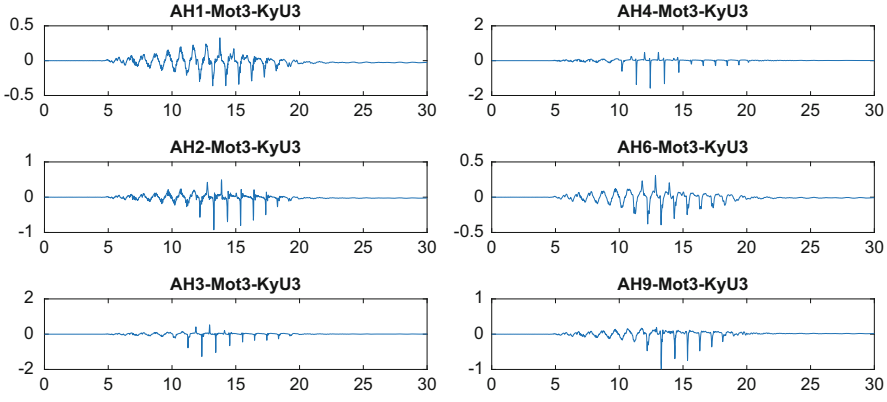

Fig. 17.15 Ground motion accelerations (g) versus time (s) for Model KyU3—Motion 3

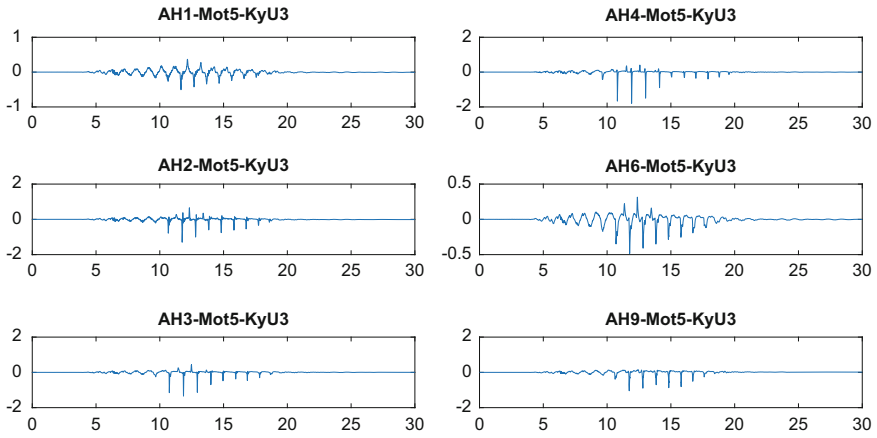

Fig. 17.16 Ground motion accelerations (g) versus time (s) for Model KyU3—Motion 5

bottom accelerometers (i.e. AH1, AH2). However, for accelerometers AH3, AH4, AH6, and AH9, initially, the recorded acceleration remained similar to the input motion before the development of significant EPWP (at around 13 s); after that, the motion significantly changed and developed sharp spikes (which are characteristic of a dilative behavior of liquefied sand). It is important to remark that the distortion in the acceleration starts first (and also becomes larger) with a decrease in effective vertical stress, because the EPWP generation developed faster in those zones.

For Motions 3 and 5 (Figs. 17.11, 17.12, 17.15 and 17.16), the input wave is similar and greater than in Motion 2 and the recorded response of all accelerometers is similar to the response of accelerometers AH3, AH4, AH6, and AH9 in Motion 2. However, the start of distortion in the response waves starts sooner (due to the increase in the PGA), at around 10 s for the shallow accelerometers.

17.3.4 Cone Penetration Tests

As specified, cone penetration tests (CPTs) were performed before each destructive motion; hence, CPT1, CPT2, and CPT3 were performed before Motions 2, 3, and 5, respectively.

Figures 17.17a and 17.17b shows the penetration test results for each model; in Model KyU2 penetration tests, no significant differences were obtained among CPT 1 and CPT 2; for CPT3 an increase between 20 and 30% in the value of qc is reported, so an increase in the liquefaction resistance would be reasonable; however, as explained before, little difference was found in the values of EPWP, between Motions 3 and 5. Yamada et al. (2010) found that in the case of re-liquefaction process (i.e. multiple liquefaction process in the same ground), anisotropy of soils becomes a key factor, rather than the relative density. This fact may explain the

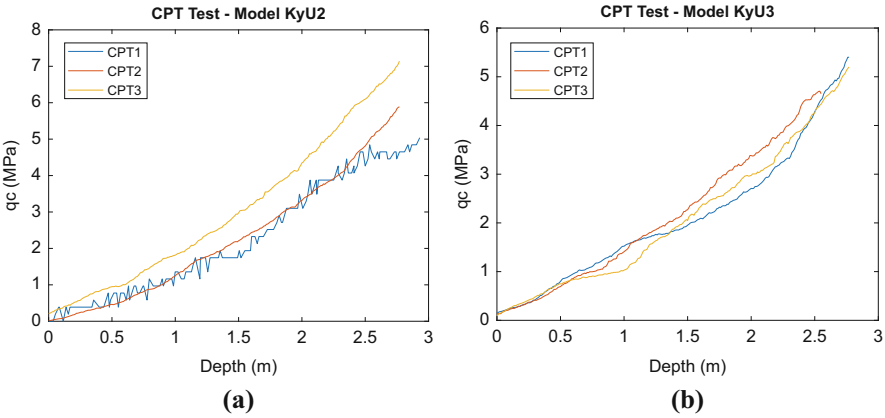

Fig. 17.17 (**a**) CPT test results for model KyU2 (**b**) CPT test results for model KyU3

similar behavior in the development of EPWP in Motions 3 and 5 for Model KyU2, even when the q_c value became larger prior Motion 5.

For Model KyU3, no significant differences were found among the three CPT realizations; also, as the previous case, no significant difference was found in the values of EPWP, between Motion 3 and 5.

It is also worth to mention that due to the characteristics of the CPT apparatus, it was not possible to perform shaking while the apparatus was mounted; consequently, each time the CPT tests were performed, the centrifuge had to: (1) be stopped to assemble the CPT, (2) increase the g-level at 44.4 g to perform the test, (3) stop again the facility to disassemble the CPT, and (4) increase the g-level for the shaking process. Effects of this procedure on soil density should be quantified in the future.

17.4 Discussion of Special Features

17.4.1 Sensitivity of Density Measurement by Volumetric Methods

As indicated in Sect. 17.2.2, density was measured at three different stages in each model (as shown in Fig. 17.18), and variability among each layer was found. It is important to remark that models were prepared as a "flat ground" by air pluviation, and density measurements were performed during this process; the curved surface was obtained thereafter by applying vacuum (as stated in Sect. 17.2.2).

Taking into account that the dimensions of the rigid box that were used for both models are L = 45 cm, W = 15 cm, and H = 31 cm, Fig. 17.19 shows a very simple sensitivity analysis that was performed to estimate the limits of the Dr values that

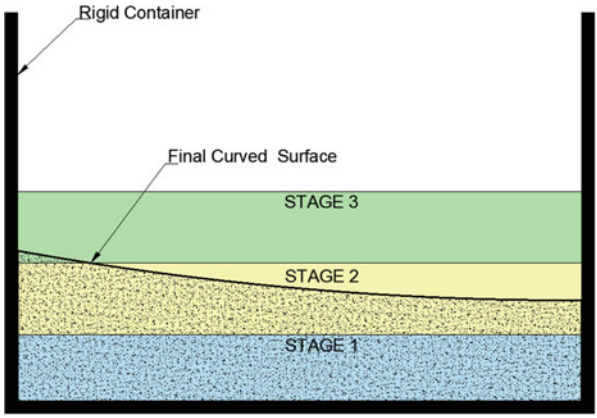

Fig. 17.18 Stages of air pluviation procedure and density measurement

could be achieved if a measurement error would be committed. According to Fig. 17.18, the achieved density of sand placed in Stages 1 and 2 covers more than 99% of the final curved surface, so stage 3 is not presented.

For the sensitivity analysis due to the conditions of the experiment, weight of sand, and depth and width dimensions of the container were taken as constant values, and the measurement of the height of pluviated sand was taken as a variable. It is important to mention that, for each density measurement, height of sand was measured at 15 uniformly distributed points over the surface of ground; with this information, dry density was calculated as the ratio of weight to volume.

As seen in Fig. 17.19 for Stage 1, an error in the measurement of the height of sand of just 1 mm would lead to a constant deviation in the Dr value of 10% (Fig. 17.19a), which for some analysis may be considered as an important deviation. For the same 1 mm error in the height of sand, if we are interested in the measurement of density for only Stage 2, the deviation in the Dr value would remain the same; however, if we want to estimate the overall average density, the deviation associated with 1 mm height error would be reduced to 5% (Fig. 17.19b).

With regard to the achieved measurements of the sand's height, values ranging from 10% (for Stage 1 measurements) to 3% (for Stage 2 measurements) correspondent to the "coefficient of variability" (i.e. standard deviation normalized by the mean value) were obtained; it seems that this variability was mainly caused by the "edge effect," which led to obtain lower surface values near the container's edges during the air pluviation procedure.

Figure 17.20 shows the results for an air pluviation calibration exercise (20 trials were performed and each point corresponds to the average of 3 or 4 trials) realized prior the development of models. A strong correlation was not obtained ($r^2 \approx 0.68$), which lead us to think that homogeneity may not be ensured in the whole process.

The causes of the nonachievement of strong correlation were not still fully determined; but one important reason may be that the container selected for air pluviation (as shown in Fig. 17.2) produced a "high" volume flow of sand during the

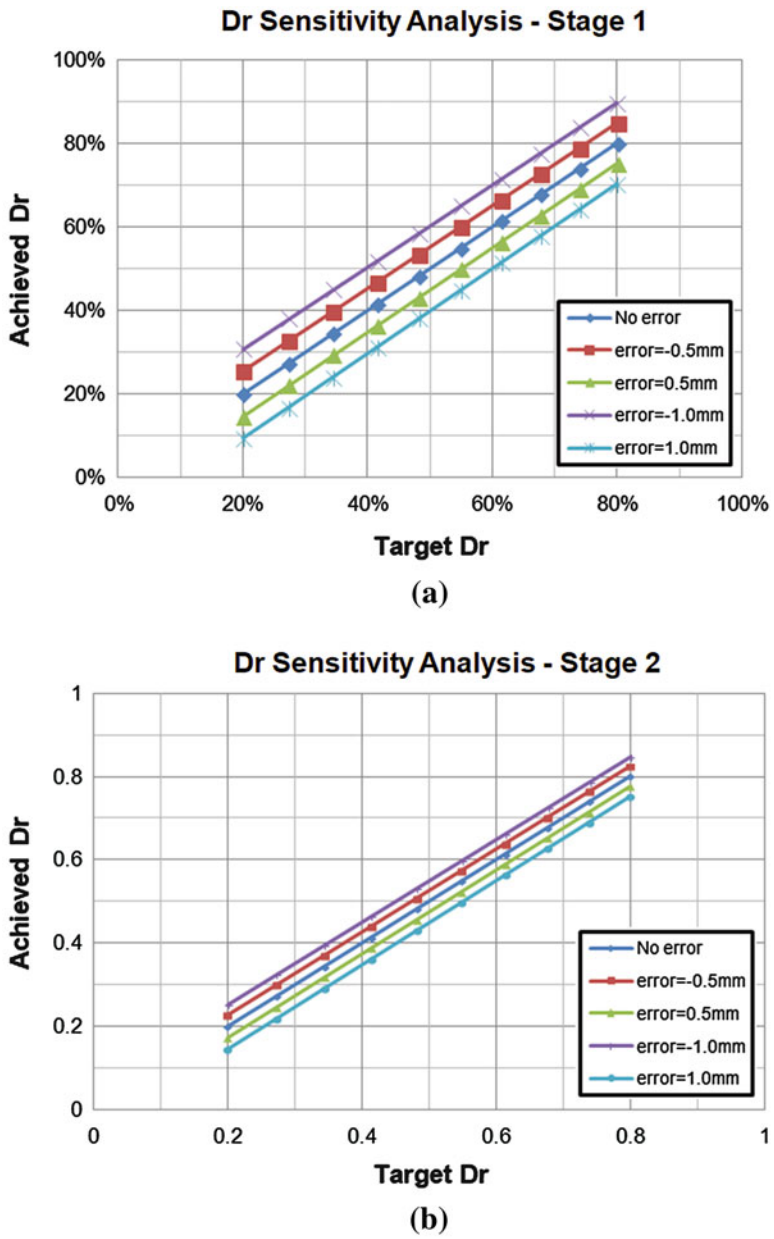

Fig. 17.19 (**a**) Sensitivity analysis for density measurement—stage 1. (**b**) Sensitivity analysis for density measurement—stage 2

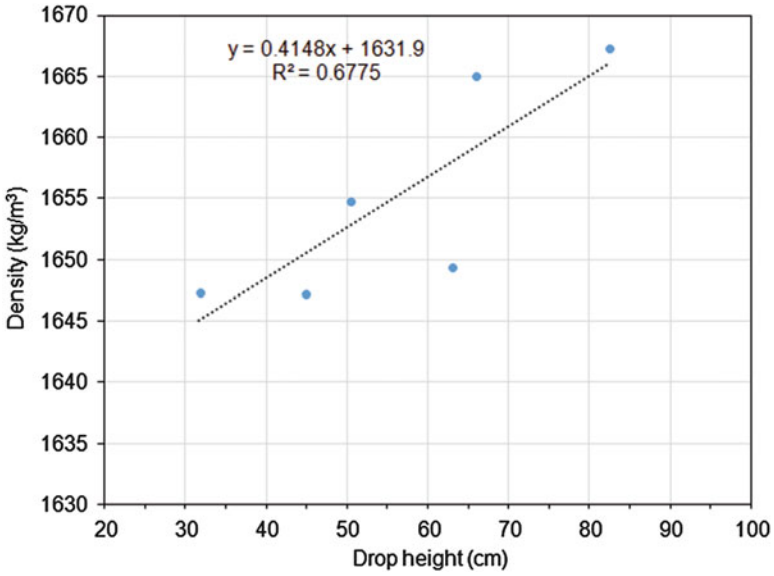

Fig. 17.20 Drop height calibration for the air pluviation process

process. T his caused that in some intervals of time, an horizontal and uniform surface was not kept (increasing the "edge effect"). Therefore, decreasing the volume flow (i.e. reducing the area of each hole, or keeping one hole instead of three) could be a possibility to improve the correlation degree and homogeneity.

17.4.2 Correlation Between CPT and Density Measurements

As described in previous sections for the characteristics of this project, measured density values seem to be very sensitive to measurements of volume. Therefore, in this section a comparison of density obtained by the "mass–volume measurements" and density obtained from "correlations from CPT" is performed.

As described in Sect. 17.3.4, three CPT tests were performed per each model; in this section, in order to analyze the initial density, results obtained just in the first CPT of each model at depths between 1.5 and 2.5 m are discussed. An empirical correlation (provided by UC Davis) between dry density and q_c is employed for comparative purposes; this correlation has the form: $\rho_{dry} = a \times q_c + b$, where ρ_{dry} is the dry density obtained by the correlation, q_c is the tip resistance measured at CPT test, and "a" and "b" are depth dependent constants determined by linear regression between qc and density at a particular depth of measurement of q_c. The a and b values were provided at three depths (1.5, 2, and 2.5 m) in a spreadsheet described by Kutter et al. (2019). A quadratic curve fit was used to interpolate a and b values at intermediate depths; using this interpolated values, it was then possible to obtain a

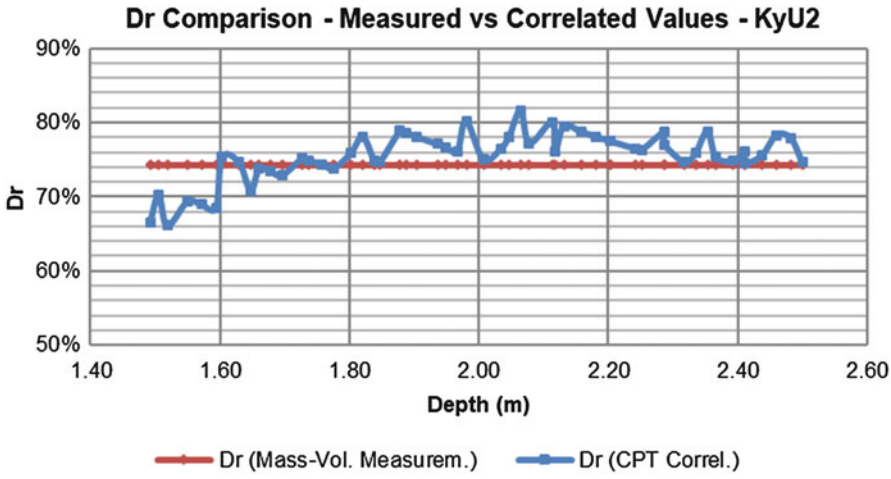

Fig. 17.21 Comparison between the achieved Dr values obtained by "correlations from CPT" and "mass–volume measurements" for KyU2 Model

continuous estimate of the "correlated" density. Figures 17.21 and 17.22 show a comparison between the achieved Dr values obtained by "correlations from CPT" and "mass–volume measurements" for the KyU2 and KyU3 Models, respectively.

Figure 17.21 shows that on average, there is no significant difference in the Dr values obtained by the two different methods; however, Fig. 17.22 shows a difference of 4% on average. A more formal definition of the weighted average deviation between the correlated relative density and the measured relative density was determined using the Δ_{D_r} value, which was estimated as follows.

$$\Delta_{\mathrm{Dr}} = \frac{\sum_{i=1}^{n}\left[(d_i - d_{i-1}) \cdot \left(\frac{\left|\mathrm{Dr}_m - \mathrm{Dr}_{c_i}\right| + \left|\mathrm{Dr}_m - \mathrm{Dr}_{c_{i-1}}\right|}{2}\right)\right]}{d_n - d_0}$$

where:

- Δ_{Dr}: Weighted average of difference between "measured Dr" and "correlated Dr"
- d_i: Depth of CPT on the ith measurement
- Dr_m: Measured relative density
- Dr_{c_i}: Estimated relative density on the ith measurement (based on q_c values)
- n: Number of CPT measurements in each test

The weighted average Δ_{Dr} values were tabulated for all of the LEAP-UCD-2017 centrifuge tests for which CPT data was available. The distribution of the average deviation is summarized in Fig. 17.23. It can be seen that in most cases the Δ_{Dr} was less than 5%, but in 26% of the cases the deviation was more than 5%.

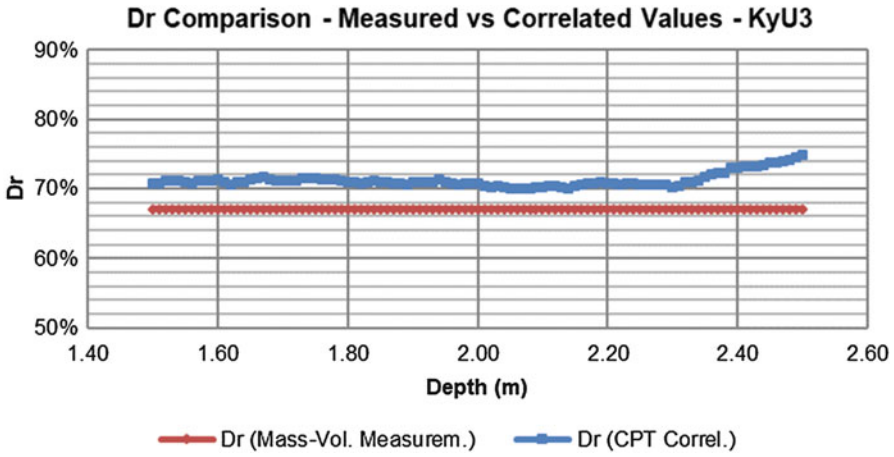

Fig. 17.22 Comparison between the achieved Dr values obtained by "correlations from CPT", and "mass–volume measurements" for KyU3 Model

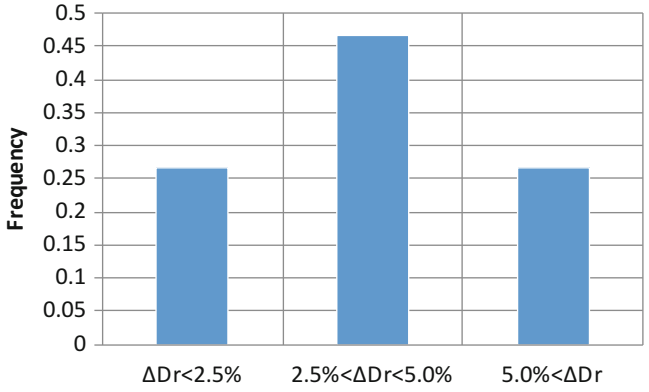

Fig. 17.23 Distribution of Δ_{Dr} value among facilities

17.5 Conclusions

LEAP (Liquefaction Experiments and Analysis Projects) is a joint exercise that pursues the verification, validation, and uncertainty quantification of numerical liquefaction models. "LEAP-UCD-2017" is one of the LEAP's exercises, whose main objective is to perform a sufficient number of experiments to characterize the median response, and the uncertainty of response of a specific sloping deposit of sand.

A review of the KyU2 and KyU3 Models performed in the facilities of the Disaster Prevention Research Institute at Kyoto University for "LEAP-UCD-2017" exercise was presented.

- A brief review of the specifications for the realizations was explained, along with the characteristics and differences performed to obtain the "as-built" model.
- For both models, results of excess of pore water pressure in Motion 2 (PGA 0.15) showed values of $r_u \approx 1$ in shallow sensors; however, for Motions 3 and 5 (PGA 0.25), values of $r_u \approx 1$ were obtained almost in all of the sensors.
- For Model KyU2, despite the increase in the values of q_c (obtained through the CPT test before Motion 3, and before Motion 5), no increase in liquefaction resistance was observed; these values are in accordance with the values obtained by Yamada et al. (2010), who found that in the case of re-liquefaction process, anisotropy of soils becomes a key factor, rather than the relative density.
- Relating to ground motion accelerations, as expected the recorded acceleration remained similar as the input motion before the development of significant EPWP; thereafter, significant distortion was recorded, presenting sharp spikes which are characteristic from dilatant behavior of liquefied soil.

Due to its importance in verification & validation tests, a discussion about density measurement was presented in Sect. 17.4.

- Volumetric measurement of density becomes very sensitive (even for small errors); therefore, special attention should be focused on this step in future experiments.
- Specified container for "air pluviation" may be checked for further experiments; size of the apertures might be reviewed to reduce the volume flow of sand, in order decrease the dependence on the operator's ability to keep horizontal and uniform surface during air pluviation.
- Comparison of density values obtained by correlations with CPT tests and by mass and volume measurements shows a discrepancy among research facilities. To reduce the discrepancy in future LEAP exercises, it is recommended that increased attention be devoted to improving the accuracy of density measurements by both methods.

References

Izumo, N. (2006). Physical quantity measured by a vibration viscometer. In *Proceedings of 23th Sensing Forum, Tsukuba*. pp. 149–152.

Kutter, B. L., Carey, T. J., Stone, N., Bonab, M. H., Manzari, M., Zeghal, M., Escoffier, S., Haigh, S., Madabhushi, G., Hung, W.-Y., Kim, D.-S., Kim, N.-R., Okamura, M., Tobita, T., Ueda, K., & Zhou, Y.-G. (2019). LEAP-UCD-2017 V. 1.01 model specifications. In B. Kutter et al. (Eds.), *Model tests and numerical simulations of liquefaction and lateral spreading: LEAP-UCD-2017*. New York: Springer.

Okamura, M., & Inoue, T. (2012). Preparation of fully saturated models for liquefaction study. *International Journal of Physical Modeling in Geotechnics, 12*(1), 39–46. https://doi.org/10.1680/ijpmg.2012.12.1.39.

Tobita, T., Ashino, T., Ren, J., & Iai, S. (2018). Kyoto University LEAP-GWU-2015 tests and the importance of curving the ground surface in centrifuge modelling. *International Journal of Soil Dynamics and Earthquake Engineering, 113*, 650–662. https://doi.org/10.1016/j.soildyn.2017.10.012.

Yamada, S., Takamori, T., & Sato, K. (2010). Effects on reliquefaction resistance produced bu changes in anisotropy during liquefaction. *Soils and Foundations, 50*(1), 9–25.